Progress In Electromagnetics Research B, Vol. 8, 1–28, 2008

SPATIOTEMPORALLY LOCALIZED NULL ELECTROMAGNETIC WAVES I. LUMINAL[†]

I. M. Besieris

Bradley Department of Electrical and Computer Engineering
Virginia Polytechnic Institute and State University
Blacksburg, VA 24060, USA

A. M. Shaarawi

Department of Physics
The American University of Cairo
P.O. Box 2511, Cairo 11511, Egypt

Abstract—Spatiotemporally localized luminal null electromagnetic fields are transverse with respect to the local flow of energy, which is equipartioned between the electric and magnetic fields, and the modulus of their local energy transport velocity equals the speed of light in vacuo. They have vortex structures on planes transverse to the direction of propagation, and, in general, are relatively simple so that explicit calculations can be made of the total energy and the total angular momentum they carry. A class of luminal null electromagnetic waves due originally to Robinson and Troutman is motivated by means of spherical Cunningham and Bateman transformations and their relationships to well-known scalar luminal localized waves are examined. This allows for the introduction of finite-energy localized null luminal electromagnetic waves with spatiotemporal spectra appropriate for applications in diverse physical areas.

1. INTRODUCTION

The current interest in linear luminal spatiotemporally localized waves (LWs) was initiated by the pioneering contributions of Brittingham [1] and Kiselev [2], who introduced one class of LWs, the focus wave mode (FWM), and by the subsequent refinements of the underlying theory

[†] Dedicated to the memory of Jin Au Kong.

by Belanger [3], Ziolkowski [4,5], Besieris, Shaarawi and Ziolkowski [6, 7] and others. This interest has been sustained by advancements in ultrafast acoustical, optical, and electrical devices capable of generating and shaping very short pulsed wave fields (see, e.g., [8]) and by the prospects of using LW fields in diverse applications, such as nondestructive testing, ultrafast microscopy, high resolution imaging, tissue characterization and photodynamic therapy. Experimental validation of luminal LW phenomena has been carried out in the acoustical [9, 10] and optical [11] frequency regimes.

A very general class of luminal LW solutions to the (3+1)-dimensional homogeneous scalar wave equation in free space, viz.,

$$\left(\nabla^2 - \frac{1}{c^2}\frac{\partial^2}{\partial t^2}\right)\psi(\vec{r},t) = 0; \quad \vec{r} \equiv \{x,y,z\}, \tag{1}$$

is given as follows:

$$\begin{aligned} \psi(\vec{r},t) &= \frac{1}{a_1 + i(z-ct)} f(\alpha,\beta); \\ \alpha(\vec{r},t) &\equiv a_2 - i(z+ct) + \frac{x^2+y^2}{a_1+i(z-ct)}, \\ \beta(\vec{r},t) &\equiv \frac{x-iy}{a_1+i(z-ct)}. \end{aligned} \tag{2}$$

Here, c denotes the speed of light *in vacuo*, $a_{1,2}$ are free positive parameters, and $f(\cdot)$ is an arbitrary function. A number of observations regarding the class of solutions incorporated into Eq. (2) will be made next.

1) These solutions obey the Courant-Hilbert *ansatz* [12], which states that "relatively undistorted" progressive solutions to the scalar wave equation (1) assume the form

$$\psi(\vec{r},t) = g(\vec{r},t) f[\theta(\vec{r},t)], \tag{3}$$

where $f(\cdot)$ is essentially an arbitrary function, $\theta(\vec{r},t)$, referred to as the "phase" function, obeys the nonlinear characteristic equation

$$(\partial\theta/\partial x)^2 + (\partial\theta/\partial y)^2 + (\partial\theta/\partial z)^2 - (1/c^2)(\partial\theta/\partial t)^2 = 0, \tag{4}$$

and $g(\vec{r},t)$ is an "attenuation" function, the latter depending on $\theta(\vec{r},t)$, but not in a unique manner. For the class of solutions given in Eq. (2), the attenuation function is given by $g(\vec{r},t) = [a_1 + i(z-ct)]^{-1}$.

2) In 1992, Hillion [13] recognized that luminal LWs of the form given in Eq. (2), but in the absence of $\beta(\vec{r},t)$ entering into the argument

of the function $f(\cdot)$, could be derived by complexification of real-valued solutions obtained by means of four-dimensional conformal transformations introduced by Bateman [14, 15].

3) The appearance of the function $\beta(\vec{r},t)$ in Eq. (2) is due to more recent work by Borisov and Utkin [16] and Kiselev [17] based on a technique combining the method of incomplete separation of variables and Bateman's four-dimensional conformal transformations (see, also, [18]).

4) The wave functions in Eq. (2) are clearly *bidirectional* due to the presence of the two characteristic variables $z-ct$ and $z+ct$ of the $(1+1)-D$ scalar wave equation. However, the parameters $a_{1,2}$, as well as additional free parameters entering through the function $f(\cdot)$ in Eq. (2), can be "tweaked" so that the wave packets can propagate primarily in the positive z direction. Very close replicas of such LWs can be launched causally from apertures constructed on the basis of the Huygens principle [19, 20].

5) Depending on the choice of the function $f(\cdot)$ in Eq. (2), the resulting luminal LWs may have either infinite or finite energy content. The former propagate along the positive z direction with only local deformations; more precisely, they regenerate periodically. The latter, on the other hand, can have extended ranges of localization in the near-to-far regions. In general, the axial localization near the pulse center is algebraic and the transverse localization is exponential. However, Kiselev [21] has shown that certain wave packets may possess both axial and transverse exponential localization.

6) A variant of the solution in Eq. (2) is the following:

$$\begin{aligned}
\psi(\vec{r},t) &= \frac{1}{a_2 - i(z+ct)} f(\overline{\alpha},\overline{\beta});\\
\overline{\alpha}(\vec{r},t) &\equiv a_1 + i(z-ct) + \frac{x^2+y^2}{a_2 - i(z+ct)},\\
\overline{\beta}(\vec{r},t) &\equiv \frac{x+iy}{a_2 - i(z+ct)}.
\end{aligned} \tag{5}$$

An interesting aspect of this solution is that with the formal substitution $z+ct \to 2z$, the function

$$\begin{aligned}
\psi_{PB}(\vec{r},t) &= \frac{1}{a_2 - i2z} f(\hat{\alpha},\hat{\beta});\\
\hat{\alpha}(\vec{r},t) &\equiv a_1 + i(z-ct) + \frac{x^2+y^2}{a_2 - i2z},\\
\hat{\beta}(\vec{r}) &\equiv \frac{x+iy}{a_2 - i2z}
\end{aligned} \tag{6}$$

obeys the *pulsed beam equation* [22]

$$\left(\frac{\partial^2}{\partial x^2}+\frac{\partial^2}{\partial y^2}+2\frac{\partial^2}{\partial \varsigma \partial z}\right)\psi_{PB}(\vec{r},t)=0; \quad \varsigma \equiv z-ct, \tag{7}$$

which, in turn, is the paraxial approximation of the scalar wave equation (1).

A brief summary has been provided so far of some of the developments in the area of luminal LWs stemming from the seminal work of Brittingham [1] and Kiselev [2] in 1983. However, a different path to certain types of luminal (FWM-type) LWs has been followed which seems to have been unknown to the aforementioned researchers until recently. In 1909 and 1910, Cunningham [23] and Bateman [24, 25] discovered a class of transformations, more general than conformal changes of the metric, which could be used to transform solutions of Maxwell's equations into similar ones. Their work became the precursor of an elaborate theory of manifolds developed originally by Robinson [26] and extended by Robinson and Trautman [27–29]. The Robinson-Trautman theory has played a significant role in general relativity, as well as in other areas of physics (e.g., Penrose twistor theory [30]). It turns out that one family of the Robinson-Trautman solutions includes an extremely appealing FWM-type null solution to Maxwell's equations. This important aspect has been brought out in the recent work on electromagnetic vortices by Bialynicki-Birula [31].

The Robinson-Troutman luminal null electromagnetic LW cannot be derived easily by conventional means, e.g., by using a scalar luminal LW $\psi(\vec{r},t)$ from the general class in Eq. (2) to form an electric or a magnetic Hertz vector potential. Our first aim in this paper is to motivate the Robinson-Troutman luminal null electromagnetic LW through spherical Cunningham and Bateman transformations. Subsequently, a relationship is established between the Robinson-Troutman luminal null electromagnetic LW and a specific scalar luminal LW known as the third-order splash mode. This relationship is extended so that a correspondence can be created between any luminal null electromagnetic LW and a scalar luminal LW from the general class of solutions given in Eq. (2).

The salient features of the Robinson-Trautman luminal null electromagnetic LW introduced by Bialynicki-Birula [31] are discussed in Section 2. A systematic derivation of the Robinson-Troutman luminal null electromagnetic LW, as well as a broader class of finite energy luminal null electromagnetic LWs, based on Cunningham and Bateman spherical transformations is provided in Section 3. Spatiotemporally localized null electromagnetic pulsed beams are discussed in Section 4. Concluding remarks are made in Section 5.

2. THE ROBINSON-TROUTMAN LOCALIZED LUMINAL NULL ELECTROMAGNETIC WAVE

2.1. The Riemann-Silberstein Vector

The Robinson-Trautman luminal null electromagnetic LW, as introduced by Bialynicki-Birula [31], is most conveniently expressed in terms of a complex-valued vector first used by Riemann [32] and afterwards by Silberstein [33]. Let $\vec{E}(\vec{r},t)$ and $\vec{H}(\vec{r},t)$ denote respectively the real-valued electric and magnetic field intensities satisfying the homogeneous Maxwell equations in free space, viz.,

$$\begin{aligned} \nabla\times\vec{E} &= -\mu_0\frac{\partial}{\partial t}\vec{H}, \\ \nabla\times\vec{H} &= \varepsilon_0\frac{\partial}{\partial t}\vec{E}, \\ \nabla\cdot\vec{E} &= 0, \quad \nabla\cdot\vec{H}=0, \end{aligned} \tag{8}$$

where ε_0 and μ_0 are the electric permittivity and magnetic permeability of vacuum, respectively. Then, the complex-valued Riemann-Silberstein vector is defined as follows:

$$\vec{F} = \sqrt{\frac{\varepsilon_0}{2}}\vec{E} + i\sqrt{\frac{\mu_0}{2}}\vec{H}. \tag{9}$$

It obeys the equations

$$\nabla\times\vec{F} = -i\frac{1}{c}\frac{\partial}{\partial t}\vec{F}, \qquad \nabla\cdot\vec{F}=0, \tag{10}$$

which are precisely equivalent to the original Maxwell equations (8). Certain important physical quantities associated with the real fields $\vec{E}(\vec{r},t)$ and $\vec{H}(\vec{r},t)$ can be expressed conveniently in terms of $\vec{F}(\vec{r},t)$. Specifically, the Poynting vector and the electromagnetic field energy density can be written as

$$\begin{aligned} \vec{P} &= \vec{E}\times\vec{H} = -ic\vec{F}^*\times\vec{F}, \\ w_{em} &= \frac{\varepsilon_0}{2}\vec{E}\cdot\vec{E} + \frac{\mu_0}{2}\vec{H}\cdot\vec{H} = \vec{F}^*\cdot\vec{F}, \end{aligned} \tag{11}$$

respectively.

2.2. The Robinson-Trautman Localized Luminal Null Electromagnetic Wave

Recall the functions $\alpha(\vec{r},t)$ and $\beta(\vec{r},t)$ defined in Eq. (2), viz.,

$$\alpha(\vec{r},t) \equiv a_2 - i(z+ct) + \frac{x^2+y^2}{a_1+i(z-ct)}, \quad \beta(\vec{r},t) \equiv \frac{x-iy}{a_1+i(z-ct)}. \tag{12}$$

Then, the Riemann-Silberstein vector associated with the Robinson-Trautman luminal electromagnetic LW, as introduced by Bialinicki-Birula [31], is given as follows:

$$\vec{F}_{RT} = \left\{ \frac{1}{\alpha^3}\frac{-\beta^2-1}{a_1+i(z-ct)}, i\frac{1}{\alpha^3}\frac{-\beta^2+1}{a_1+i(z-ct)}, i\frac{1}{\alpha^3}\frac{2\beta}{a_1+i(z-ct)} \right\}. \tag{13}$$

In order to relate this expression to other work in the area of luminal localized waves, a *basic vector* is defined as

$$\vec{f_b} = \{-(1+\beta^2), i(1-\beta^2), 2i\beta\} \tag{14}$$

and the Robinson-Troutman Riemann-Silberstein vector is rewritten as follows:

$$\vec{F}_{RT}(\vec{r},t) = \frac{1}{a_1+i(z-ct)}\frac{1}{\alpha^3}\vec{f_b}(\vec{r},t). \tag{15}$$

The function multiplying the basic vector on the right-hand side of this equation is the third-order *splash mode*. The latter belongs to a special class of finite-energy luminal LWs introduced by Ziolkowski [4].

An important aspect of $\vec{F}_{RT}$ is that it obeys the *null* property; specifically, that there exists a vector $\vec{n}$, such that $\vec{F}_{RT} = -i\vec{n}\times\vec{F}_{RT}$. It follows, then, that $\vec{F}_{RT}\cdot\vec{F}_{RT} \equiv 0$. The physical significance of the nullity condition will be discussed in detail later on.

Each of the components of $\vec{F}_{RT}$ conforms to the general template given in Eq. (2) for luminal (FWM-type) localized solutions to the scalar wave equation (1). As a consequence, the real fields

$$\vec{E} = \sqrt{\frac{2}{\varepsilon_0}}\mathrm{Re}\left\{\vec{F}_{RT}\right\}, \quad \vec{H} = \sqrt{\frac{2}{\mu_0}}\mathrm{Im}\left\{\vec{F}_{RT}\right\} \tag{16}$$

are endowed with the spatiotemporal localization properties discussed in Section 1. As pointed out by Bialynicki-Birula [31], the real fields corresponding to the Riemann-Silberstein vector in Eq. (13) contain finite total energy and have finite total axial angular momentum;

specifically,

$$\begin{aligned} \text{Total Energy} &= \int\limits_{R_3} d\vec{r} w_{em}(\vec{r},t) = \frac{\pi^2}{4a_1^5}, \\ \text{Total Angular Momentum} &= \frac{1}{c^2}\int\limits_{R_3} d\vec{r}\vec{r}\times\vec{P} = \frac{5\pi^2}{16a_1^6}\hat{z}, \end{aligned} \tag{17}$$

in the special case where $a_1 = a_2$. The total transverse angular momentum vanishes.

A number of graphical results are presented next in order to obtain a clearer view of some of the unique features of the Robinson-Trautman null luminal electromagnetic LW. The following notation is used: $\tau \equiv t - z/c$ is the local time coordinate around the pulse center; therefore, z is the distance from an "aperture" located at $z = 0$. The parameter values for all figures are $a_1 = 10^{-4}$ m and $a_2 = 10^4$ m Fig. 1(a) is a plot of $|E_x|$ vs. x, y for $\tau = -5 \times 10^{-13}, 0$ and 5×10^{-13} s on the aperture plane ($z = 0$). An antisymmetric "helical" structure to

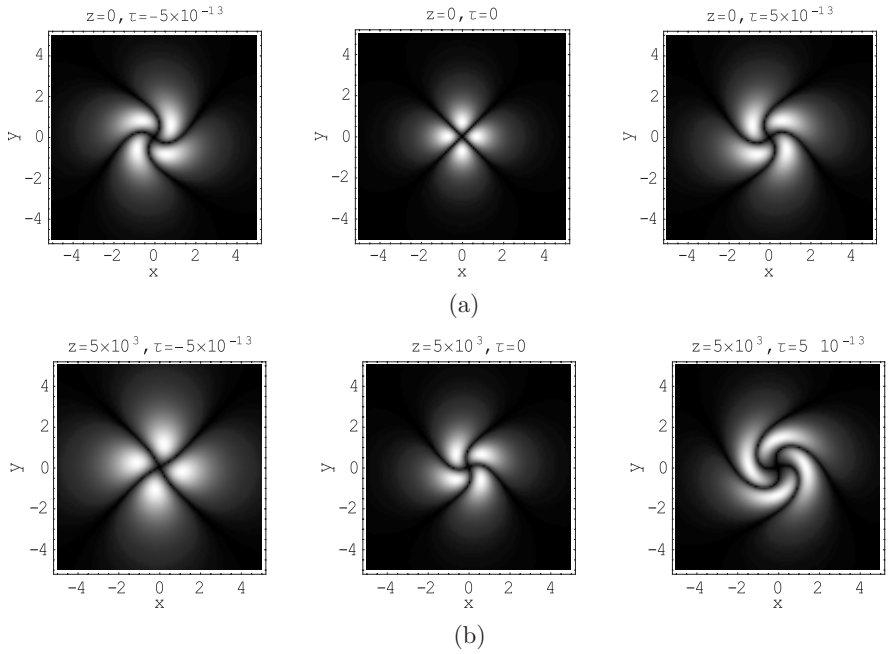

Figure 1. (a) $|\vec{E}_x|$ vs. x, y for $\tau = -5 \times 10^{-13}, 0$ and 5×10^{-13} s at $z = 0$. (b) $|\vec{E}_x|$ vs. x, y for $\tau = -5 \times 10^{-13}, 0$ and 5×10^{-13} s at $z = 5 \times 10^3$ m; Parameter values: $a_1 = 10^{-4}$ m, $a_2 = 10^4$ m.

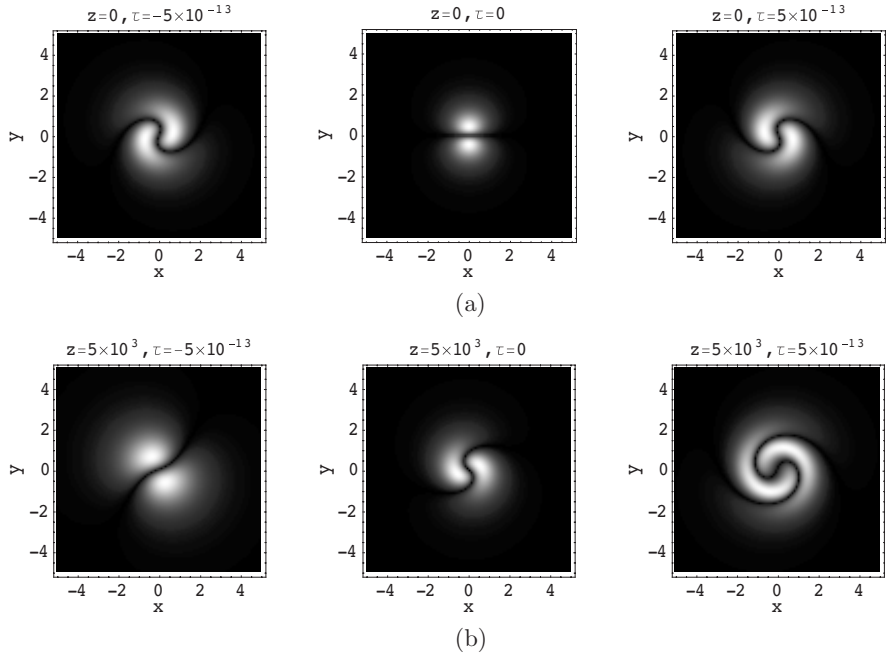

Figure 2. (a) $|\vec{E}_z|$ vs. x, y for $\tau = -5 \times 10^{-13}, 0$ and 5×10^{-13} m at $z = 0$. (b) $|\vec{E}_z|$ vs. x, y for $\tau = -10^{-13}, 0$ and 10^{-13} s at $z = 5 \times 10^3$ m; Parameter values: $a_1 = 10^{-4}$ m, $a_2 = 10^4$ m.

the left and the right of the pulse center is clearly evident. Fig. 1(b) is a plot of $|E_x|$ vs. x, y for $\tau = -5\times10^{-13}, 0$ and 5×10^{-13} s at $z = 5\times10^3$ m. The different behavior at the pulse center and the loss of symmetry to the left and the right of the pulse center is due to the deformation of the wave packet as it propagates away from the aperture plane. A similar, but distinct, behavior is exhibited in Figs. 2(a) and 2(b) for $|E_z|$. Despite the lack of azimuthal symmetry for the electromagnetic fields, the electromagnetic field energy density, shown in Fig. 3, is axisymmetric. The presence of an axial angular momentum is clearly seen in Fig. 4(a), which shows a plot of the electromagnetic momentum density $(1/c^2)\vec{E} \times \vec{H}$ vs. x, y for $\tau = -5 \times 10^{-13}, 0$ and 5×10^{-13} s on the aperture plane ($z = 0$). Parametric field plots of the x- and y-components of the angular momentum density $\vec{r} \times (\vec{E} \times \vec{H})/c^2$ vs. x, y for $\tau = -5 \times 10^{-13}, 0$ and 5×10^{-13} s on the aperture plane ($z = 0$) are shown in Fig. 4(b).

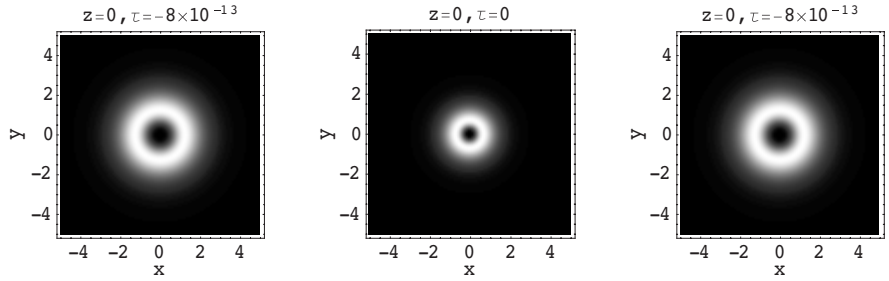

Figure 3. Electromagnetic field energy density w_{em} vs. x, y for $\tau = -8 \times 10^{-13}, 0$ and 8×10^{-13} s at $z = 0$; Parameter values: $a_1 = 10^{-4}$ m, $a_2 = 10^4$ m.

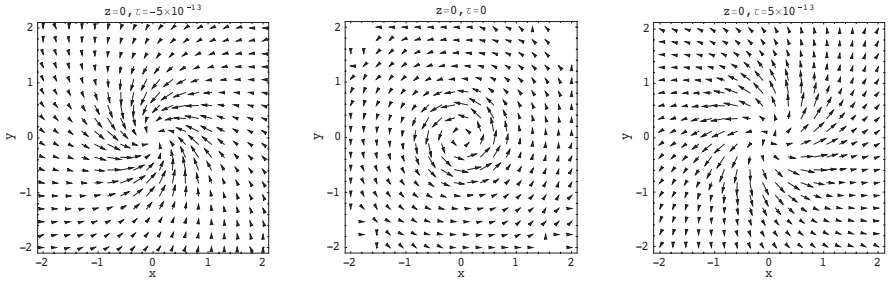

Figure 4a. Parametric field plots of the x- and y-components of the electromagnetic momentum $(1/c^2)\vec{E} \times \vec{H}$ vs. x, y for $\tau = -5 \times 10^{-13}, 0$ and 5×10^{-13} s at $z = 0$; Parameter values: $a_1 = 10^{-4}$ m, $a_2 = 10^4$ m.

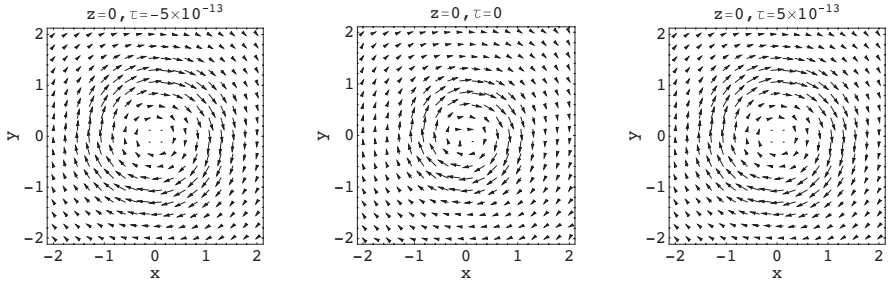

Figure 4b. Parametric field plots of the x- and y-components of the electromagnetic angular momentum density $\vec{r} \times (\vec{E} \times \vec{H})/c^2$ vs. x, y for $\tau = -5 \times 10^{-13}, 0$ and 5×10^{-13} s at $z = 0$; Parameter values: $a_1 = 10^{-4}$ m, $a_2 = 10^4$ m.

3. CUNNINGHAM AND BATEMAN APPROACHES TO LOCALIZED LUMINAL NULL ELECTROMAGNETIC WAVES

3.1. Cunningham and Bateman Spherical Transformations

In 1909 and 1910, respectively, Cunningham [23] and Bateman [24, 25] discovered classes of transformations, more general than conformal changes of the metric, which could be used to transform solutions of Maxwell's equations into similar ones. The underlying invariance does not extend to theories containing any mass scale and, in general, is violated in quantum field theories. For this reason, it has not played as significant a role in mainstream theoretical physics as the invariance of Maxwell equations under Lorentz transformations. As mentioned in Sec.1, however, the Cunningham-Bateman work motivated the Robinson-Trautman theory of manifolds [26–29], which, in turn, has been used in general relativity, as well as in other areas of physics [30]. It will be shown below that the Cunningham-Bateman theories play a pivotal role in the derivation of spatiotemporally localized luminal null electromagnetic waves.

The Cunningham spherical transformations from dimensionless space-time coordinates $\vec{r}_0 = \{x_0, y_0, z_0\},\ t_0$ to dimensionless space-time coordinates $\vec{R}_0 = \{X_0, Y_0, Z_0\},\ T_0$ are as follows:

$$\begin{aligned} X_0 &= \frac{x_0}{r_0^2 - t_0^2}, \quad Y_0 = \frac{y_0}{r_0^2 - t_0^2}, \quad Z_0 = \frac{z_0}{r_0^2 - t_0^2} \\ T_0 &= \frac{t_0}{r_0^2 - t_0^2}; \quad r_0^2 \equiv x_0^2 + y_0^2 + z_0^2. \end{aligned} \tag{18}$$

The analogous Bateman transformations are given by

$$X_0 = \frac{x_0}{z_0 - t_0},\ Y_0 = \frac{y_0}{z_0 - t_0},\ Z_0 = \frac{r_0^2 - 1 - t_0^2}{2(z_0 - t_0)},\ T_0 = \frac{r_0^2 + 1 - t_0^2}{2(z_0 - t_0)}. \tag{19}$$

The vacuum electromagnetic fields $\vec{E}(\vec{R}_0, T_0), \vec{H}(\vec{R}_0, T_0)$, with a normalized speed of light equal to unity, are transformed to the fields $\vec{e}(\vec{r}_0, t_0), \vec{h}(\vec{r}_0, t_0)$ in an identical manner in both the Cunningham and Bateman frameworks. The field components $\vec{e}_{x_0}(\vec{r}_0, t_0)$ and $\vec{h}_{x_0}(\vec{r}_0, t_0)$ are explicitly given as

$$\begin{aligned} e_{x_0} = E_{X_0} \begin{vmatrix} \partial Y_0/\partial y_0 & \partial Y_0/\partial z_0 \\ \partial Z_0/\partial y_0 & \partial Z_0/\partial z_0 \end{vmatrix} + E_{Y_0} \begin{vmatrix} \partial Z_0/\partial y_0 & \partial Z_0/\partial z_0 \\ \partial X_0/\partial y_0 & \partial X_0/\partial z_0 \end{vmatrix} \\ + E_{Z_0} \begin{vmatrix} \partial X_0/\partial y_0 & \partial X_0/\partial z_0 \\ \partial Y_0/\partial y_0 & \partial Y_0/\partial z_0 \end{vmatrix} - H_{X_0} \begin{vmatrix} \partial X_0/\partial y_0 & \partial X_0/\partial z_0 \\ \partial T_0/\partial y_0 & \partial T_0/\partial z_0 \end{vmatrix} \end{aligned}$$

$$
\begin{aligned}
&-H_{Y_0}\begin{vmatrix} \partial Y_0/\partial y_0 & \partial Y_0/\partial z_0 \\ \partial T_0/\partial y_0 & \partial T_0/\partial z_0 \end{vmatrix} - H_{Z_0}\begin{vmatrix} \partial Z_0/\partial y_0 & \partial Z_0/\partial z_0 \\ \partial T_0/\partial y_0 & \partial T_0/\partial z_0 \end{vmatrix};\\
h_{x_0} = &-E_{X_0}\begin{vmatrix} \partial Y_0/\partial x_0 & \partial Y_0/\partial t_0 \\ \partial Z_0/\partial x_0 & \partial Z_0/\partial t_0 \end{vmatrix} - E_{Y_0}\begin{vmatrix} \partial Z_0/\partial x_0 & \partial Z_0/\partial t_0 \\ \partial X_0/\partial x_0 & \partial X_0/\partial t_0 \end{vmatrix}\\
&-E_{Z_0}\begin{vmatrix} \partial X_0/\partial x_0 & \partial X_0/\partial t_0 \\ \partial Y_0/\partial x_0 & \partial Y_0/\partial t_0 \end{vmatrix} + H_{X_0}\begin{vmatrix} \partial X_0/\partial x_0 & \partial X_0/\partial t_0 \\ \partial T_0/\partial x_0 & \partial T_0/\partial t_0 \end{vmatrix}\\
&+H_{Y_0}\begin{vmatrix} \partial Y_0/\partial x_0 & \partial Y_0/\partial t_0 \\ \partial T_0/\partial x_0 & \partial T_0/\partial t_0 \end{vmatrix} + H_{Z_0}\begin{vmatrix} \partial Z_0/\partial x_0 & \partial Z_0/\partial t_0 \\ \partial T_0/\partial x_0 & \partial T_0/\partial t_0 \end{vmatrix},
\end{aligned}
\tag{20}
$$

where the symbol $|\ |$ indicates the determinant of the 2×2 Jacobian matrices. The remaining field components are obtained by means of cyclic permutations.

3.2. Cunningham and Bateman Approaches to the Robinson-Trautman Localized Luminal Null Electromagnetic Wave

3.2.1. The Cunningham Method

In the space-time frame $(\vec{R}_0, T_0)$, a specific solution to the nondimensionalized scalar wave equation

$$\left(\nabla_0^2 - \frac{\partial^2}{\partial T_0^2}\right)\varphi(\vec{R}_0, T_0) = 0 \tag{21}$$

is chosen as follows:

$$\varphi(\vec{R}_0, T_0) = (Z_0 - T_0)(X_0 - iY_0). \tag{22}$$

Next, a vector-valued magnetic Hertz potential is defined as

$$\vec{\Pi}_m(\vec{R}_0, T_0) = \left\{0, 0, \varphi(\vec{R}_0, T_0)\right\}, \tag{23}$$

and the corresponding electromagnetic field intensities are computed:

$$
\begin{aligned}
\vec{E}(\vec{R}_0, T_0) &= -\nabla_0 \times \frac{\partial}{\partial T_0}\vec{\Pi}_m(\vec{R}_0, T_0) = \{-i, -1, 0\},\\
\vec{H}(\vec{R}_0, T_0) &= \nabla_0 \times \nabla_0 \times \vec{\Pi}_m(\vec{R}_0, T_0) = \{1, -i, 0\},
\end{aligned}
\tag{24}
$$

These fields have the following interesting properties: a) They are null, i.e., $\vec{E} \cdot \vec{E} = \vec{H} \cdot \vec{H} = 0$; b) They are related to each other; specifically, $\vec{E} = i\vec{H}$.

According to the Cunningham formalism [cf. Eqs. (18) and (20)], the magnetic field intensity in the space-time frame $(\vec{r}_0, t_0)$ assumes the explicit form

$$\vec{h}(\vec{r}_0, t_0) = \left\{ \begin{array}{c} \dfrac{(z_0 - t_0)^2 - (x_0 - iy_0)^2}{\left(r_0^2 - t_0^2\right)^3} - i\dfrac{(z_0 - t_0)^2 + (x_0 - iy_0)^2}{\left(r_0^2 - t_0^2\right)^3}, \\ -2\dfrac{(z_0 - t_0)(x_0 - iy_0)^2}{\left(r_0^2 - t_0^2\right)^3} \end{array} \right\}. \tag{25}$$

It should be noted that $\vec{h} \cdot \vec{h} = 0$. Furthermore, it turns out that $\vec{e} = i\vec{h}$. This means that $\vec{e}$ is also a null field. The Robinson-Troutman Riemann-Silberstein vector given in Eq. (13) can be derived from the magnetic field intensity in Eq. (25) by means of the following space-time complexification procedure:

$$\begin{array}{l} \vec{h}(x_0, y_0, z_0, t_0) \\ \quad \Downarrow \\ x_0 \to x/k, y_0 \to y/k, z_0 \to z/k, t_0 \to ct/k; (k \sim m^{-1});\ k = 1 \\ \quad \Downarrow \\ z \to z + i\dfrac{a_1 + a_2}{2},\ ct \to ct + i\dfrac{a_1 - a_2}{2c} \\ \quad \Downarrow \\ \vec{F}_{RT}(x, y, z, t). \end{array} \tag{26}$$

3.2.2. The Bateman Method

In the space-time frame $(\vec{R}_0, T_0)$, a specific solution to the nondimensionalized scalar wave equation (21) is chosen as

$$\varphi(\vec{R}_0, T_0) = -i\frac{X_0 - iY_0}{2(Z_0 + T_0)^2}, \tag{27}$$

and a vector-valued magnetic Hertz potential is defined as in Eq. (23). The subsequent procedure leading to the Robinson-Troutman Riemann-Silberstein vector is analogous to that followed in connection with the Cunningham approach.

3.3. Implications of the Null Property

Two important physical implications of the null property will be addressed below. One deals with locally transverse electromagnetic

(TEM) fields. The second is related to vortex properties of electromagnetic fields.

For arbitrary real-valued electric and magnetic fields $\vec{E}(\vec{r},t), \vec{H}(\vec{r},t)$ in a free-space region, the local field energy transport velocity, defined as the ratio of the Poynting vector and the electromagnetic energy density, viz.,

$$\vec{v}_e(\vec{r},t) = \frac{\vec{P}(\vec{r},t)}{w_{em}(\vec{r},t)} = \frac{\vec{E}(\vec{r},t)\times\vec{H}(\vec{r},t)}{\frac{1}{2}\left[\varepsilon_0\left|\vec{E}(\vec{r},t)\right|^2+\mu_0\left|\vec{H}(\vec{r},t)\right|^2\right]}, \tag{28}$$

can be rewritten as follows:

$$\vec{v}_e(\vec{r},t) = 2c^2\frac{\vec{E}(\vec{r},t)\times\vec{B}(\vec{r},t)}{\left|\vec{E}(\vec{r},t)\right|^2+c^2\left|\vec{B}(\vec{r},t)\right|^2};\ \vec{B}(\vec{r},t)=\mu_0\vec{H}(\vec{r},t). \tag{29}$$

This form can be used to prove that $|\vec{v}_e(\vec{r},t)| \le c$. Indeed, one can obtain the relationship

$$\begin{aligned} 1-\frac{|\vec{v}_e(\vec{r},t)|^2}{c^2} &= \frac{I_1^2+4c^2I_2^2}{\left(\left|\vec{E}(\vec{r},t)\right|^2+c^2\left|\vec{B}(\vec{r},t)\right|^2\right)^2}; \\ I_1 &\equiv \left|\vec{E}(\vec{r},t)\right|^2-c^2\left|\vec{B}(\vec{r},t)\right|^2,\ I_2\equiv\vec{E}(\vec{r},t)\cdot\vec{B}(\vec{r},t). \end{aligned} \tag{30}$$

For nontrivial fields, the right hand side of Eq. (30a) is nonnegative. As a consequence $|\vec{v}_e(\vec{r},t)| \le c$.

The quantities I_1 and I_2 in Eq. (30) are invariant for the group of linear transformations which leave Maxwell's equations unaltered in form [15]. The Lorentz transformations belong to this group. Since the right-hand side of Eq. (30a) consists of the sum of two squares, the equality $|\vec{v}_e(\vec{r},t)| = c$ holds provided that both invariants $I_{1,2}$ vanish. This is ensured if the Riemann-Silberstein complex vector $\vec{F}(\vec{r},t)$ associated with the real fields $\vec{E}(\vec{r},t)$ and $\vec{H}(\vec{r},t)$ has the null property since, then, $\vec{F}(\vec{r},t)\cdot\vec{F}(\vec{r},t) = i\varepsilon_0 I_2+(\varepsilon_0/2)I_1 \equiv 0$. Under these conditions, the fields $\vec{E}(\vec{r},t)$ and $\vec{H}(\vec{r},t)$ are (physically) perpendicular to each other ($\vec{E}\cdot\vec{H}=0$) and their magnitudes are related as follows: $|\vec{H}(\vec{r},t)| = (1/\eta_0)|\vec{E}(\vec{r},t)|;\ \eta_0 \equiv \sqrt{\mu_0/\varepsilon_0}$. Furthermore, it follows from Eq. (28) that $\vec{v}_e(\vec{r},t)\cdot\vec{H}(\vec{r},t)=0$ and $\vec{v}_e(\vec{r},t)\cdot\vec{E}(\vec{r},t)=0$. Thus, the

assumption $|\vec{v}_e(\vec{r},t)| = c$ leads to the locally TEM fields

$$\begin{aligned}\vec{E}(\vec{r},t) &= \vec{E}_\perp(\vec{r},t),\\ \vec{H}(\vec{r},t) &= \vec{H}_\perp(\vec{r},t) = \frac{1}{\eta_0}\hat{a}_n(\vec{r},t)\times\vec{E}_\perp(\vec{r},t);\ \hat{a}_n(\vec{r},t)\equiv\frac{\vec{v}_e(\vec{r},t)}{c}.\end{aligned} \tag{31}$$

An additional relationship following from the null condition is given by

$$(\varepsilon_0 I_2)^2 + [(\varepsilon_0 I_1)/2]^2 = w_{em}^2 - (1/c^2)\left|\vec{P}\right|^2 \equiv 0, \tag{32}$$

which implies that $w_{em} = (1/c)|\vec{P}|$. This is tantamount to an equipartitioning of the electromagnetic energy between the electric and magnetic fields.

The *conventional* TEM fields follow from Eq. (31) under the restriction that $\hat{a}_n(\vec{r},t) = \hat{a}_n$ is a fixed unit vector. Then, both the electric and magnetic field intensities travel at the speed c in the direction $\hat{a}_n$. The energy, which is equipartitioned between the electric and the magnetic field, also is transported at the speed of light in vacuum in the same direction. Furthermore, the fields are separable with respect to the coordinates transverse to $\hat{a}_n$. The local TEM fields, on the other hand, are in general nonseparable. In addition, their energy transport speed is different at each point in space and at each instant of time. For such fields, however, $|\vec{v}_e(\vec{r},t)| = c$.

Consider, next, the product $G(\vec{r},t) = \phi(\vec{r},t)\vec{F}(\vec{r},t)$, where $\phi(\vec{r},t)$ is a complex scalar-valued function and $\vec{F}(\vec{r},t)$ is an arbitrary Riemann-Silberstein complex vector obeying Eq. (10). By virtue of the definition of $\vec{F}(\vec{r},t)$, the function $\phi(\vec{r},t)$ controls the "singularities" of the electromagnetic fields. If, for example, $\phi(\vec{r},t)$ vanishes, both the electric and magnetic field intensities vanish. The zeros of $\phi(\vec{r},t)$ define vortex lines "riding atop" of null solutions to Maxwell's equations. Assume, next, that $G(\vec{r},t) = \phi(\vec{r},t)\vec{F}(\vec{r},t)$, also, obeys Maxwell's equations, i.e.,

$$\nabla\times\vec{G} = -i\frac{1}{c}\frac{\partial}{\partial t}\vec{G},\quad \nabla\cdot\vec{G} = 0. \tag{33}$$

Bialynicki-Birula [31] has shown for such a situation that nontrivial solutions for $\phi(\vec{r},t)$ exist only if $\vec{F}(\vec{r},t)$ obeys the *null condition* $\vec{F}\cdot\vec{F} = 0$. Furthermore, the following equations must be satisfied:

$$\begin{aligned}&\frac{\partial}{\partial t}\phi(\vec{r},t) + \vec{v}_e\cdot\nabla\phi(\vec{r},t) = 0,\ \vec{F}(\vec{r},t)\cdot\nabla\phi(\vec{r},t) = 0;\\ &\vec{v}_e(\vec{r},t)\equiv\frac{-i\vec{F}^*\times\vec{F}}{\vec{F}^*\cdot\vec{F}} = \frac{\vec{E}\times\vec{H}}{w_{em}};\ w_{em}\equiv\frac{\varepsilon_0}{2}\vec{E}\cdot\vec{E} + \frac{\mu_0}{2}\vec{H}\cdot\vec{H}.\end{aligned} \tag{34}$$

Here, $\vec{E}$ and $\vec{H}$ are the real-valued fields associated with $\vec{F}$ and the vector $\vec{v}_e(\vec{r},t)$ is the "local" energy transport velocity, defined as the ratio of the Poynting vector and the electromagnetic energy density.

It is clear that the choice of a function $\phi(\vec{r},t)$ rendering the product $G(\vec{r},t) = \phi(\vec{r},t)\vec{F}(\vec{r},t)$ a Riemann-Silberstein vector depends intimately on the nature of the null vector $\vec{F}(\vec{r},t)$. For the Robinson-Troutman Riemann-Silberstein null vector $\vec{F}_{RT}(\vec{r},t)$ given in Eq. (13), a function $\phi(\vec{r},t)$ satisfying Eq. (34) is given by $\phi(\vec{r},t) = \phi(\alpha,\beta)$, where $\alpha(\vec{r},t)$ and $\beta(\vec{r},t)$ are the functions defined in Eq. (12).

3.4. Extended Localized Luminal Null Electromagnetic Waves

Based on the discussion in the previous subsection, $\vec{G}(\vec{r},t) = \phi(\alpha,\beta)\vec{F}_{RT}(\vec{r},t)$ is a complex Riemann-Silberstein complex vector for an arbitrary functional $\phi(\alpha,\beta)$ of $\alpha(\vec{r},t)$ and $\beta(\vec{r},t)$. Appropriate choices of $\phi(\alpha,\beta)$ can result in physically interesting spatio-temporally localized null luminal electromagnetic waves.

Recall Eq. (15), where $\vec{F}_{RT}(\vec{r},t)$ is written as a product of the basic vector $\vec{f}_b(\vec{r},t)$ and the third-order splash mode. At this stage, a basic Riemann-Silberstein vector is defined as follows:

$$\vec{F}_b(\vec{r},t) = \frac{1}{a_1 + i(z-ct)}\vec{f}_b(\vec{r},t). \tag{35}$$

It should be mentioned that $\vec{F}_b(\vec{r},t)$ can be derived by means of the Cunningham method described earlier starting with the dimensionless wave function $\varphi(\vec{R}_0,T_0) = -i(1/2)(X_0 - iY_0)(Z_0 - T_0)^{-2}$. The Bateman approach requires the choice $\varphi(\vec{R}_0,T_0) = i(Z_0+T_0)(X_0 - iY_0)$.

In contradistinction to $\vec{F}_{RT}(\vec{r},t)$, the complex vector $\vec{F}_b(\vec{r},t)$ has no essential localization properties. However, it will prove convenient in the sequel because it is a null vector and shares with $\vec{F}_{RT}(\vec{r},t)$ the property that $\vec{G}(\vec{r},t) = \phi(\alpha,\beta)\vec{F}_b(\vec{r},t)$ is a complex Riemann-Silberstein complex vector for an arbitrary functional $\phi(\alpha,\beta)$ of $\alpha(\vec{r},t)$ and $\beta(\vec{r},t)$.

A specific example of an extended null luminal LW, defined in terms of the Riemann-Silberstein vector

$$\vec{G}(\vec{r},t) = \phi(\alpha,\beta)\vec{F}_b(\vec{r},t), \tag{36}$$

arises from the choice

$$\phi(\alpha,\beta) \equiv \frac{1}{(a_3 + \alpha/p)^q}\exp[(b/p)\alpha]\beta^m. \tag{37}$$

In addition to a_1 and a_2, the quantities a_3, b and p are positive free parameters. For $\alpha_3 = 0,\ b = 0,\ m = 0,\ p = 1$ and $q = 3$, the function $\phi(\alpha,\beta)/[a_1+i(z-ct)]$ equals the third-order splash mode and $\vec{G}(\vec{r},t) = \vec{F}_{RT}(\vec{r},t)$. For $m = 0,\ \phi(\alpha,\beta)/[a_1 + i(z - ct)]$ is the q-order finite energy modified power spectrum (MPS) pulse, a particularly interesting scalar-valued LW introduced by Ziolkowski [4, 5]. With m arbitrary, one has an extended MPS pulse conforming to the general template in Eq. (2).

Another interesting finite-energy null luminal LW arises from the choice of the function

$$\phi(\alpha,\beta) \equiv \exp\left[ipD\sqrt{-i\alpha(\vec{r},t)} + F\right]\beta^m, \tag{38}$$

where, in addition to $a_{1,2}$ incorporated into the function $\alpha(\vec{r},t), p, D$ and F are free parameters. The expression $\phi(\alpha,\beta)/[a_1 + i(z - ct)]$ is a scalar luminal LW studied in detail by Kiselev and Perel [21]. For an appropriate choice of the parameters, the solution is analytic for all ρ, z and t, it is localized in a small vicinity of the running point $z = ct,\ \rho = 0$, and contains finite energy.

The null luminal electromagnetic LWs constructed from the Riemann-Silberstein vector $\vec{G}(\vec{r},t) = \phi(\alpha,\beta)\vec{F}_b(\vec{r},t)$ with $\phi(\alpha,\beta)$ corresponding to either the MPS pulse or the Kiselev-Perel scalar LW have their temporal spectra far removed from the origin. This constitutes a distinct advantage for the physical realizability of such solutions [11]. This is not the case for the Robinson-Troutman null LWs because they are based on scalar splash modes which, in turn, are characterized by temporal spectra that begin at the origin.

A number of graphical results are presented next in order to gain a clearer view of some of the features of the extended null luminal electromagnetic LW associated with the Riemann-Silberstein vector $\vec{G}(\vec{r},t)$ given in Eqs. (36) and (37). The following notation is used: $\tau \equiv t - z/c$ is the local temporal coordinate around the pulse center; therefore, z is the distance from an "aperture" located at $z = 0$. For all the figures, the parameter values are as follows: $a_1 = 10^{-2}\,\mathrm{m}$, $a_2 = 1,\ a_3 = 1\,\mathrm{m},\ b = 10^{14}\,\mathrm{m}^{-1},\ p = 6\times10^{15},\ q = 2$ and $m = 3$ Fig. 5(a) is a plot of $|E_x|$ vs. x, y for $\tau = -5\times10^{-11}, 0$ and $5\times10^{-11}\,\mathrm{s}$ on the aperture plane ($z = 0$). An antisymmetric "helical" structure to the left and the right of the pulse center is clearly evident. Fig. 5(b) is a plot of $|E_x|$ vs. x, y for $\tau = -5\times10^{-11}, 0$ and $5\times10^{-11}\,\mathrm{s}$ at $z = 10^{16}\,\mathrm{m}$. The invariance of the finite-energy wavepacket even at this large range away from the aperture is due to the choice of the parameter values. A similar, but distinct, behavior is exhibited in Figs. 6(a) and 6(b) for $|E_z|$. Despite the lack of azimuthal symmetry for the electromagnetic

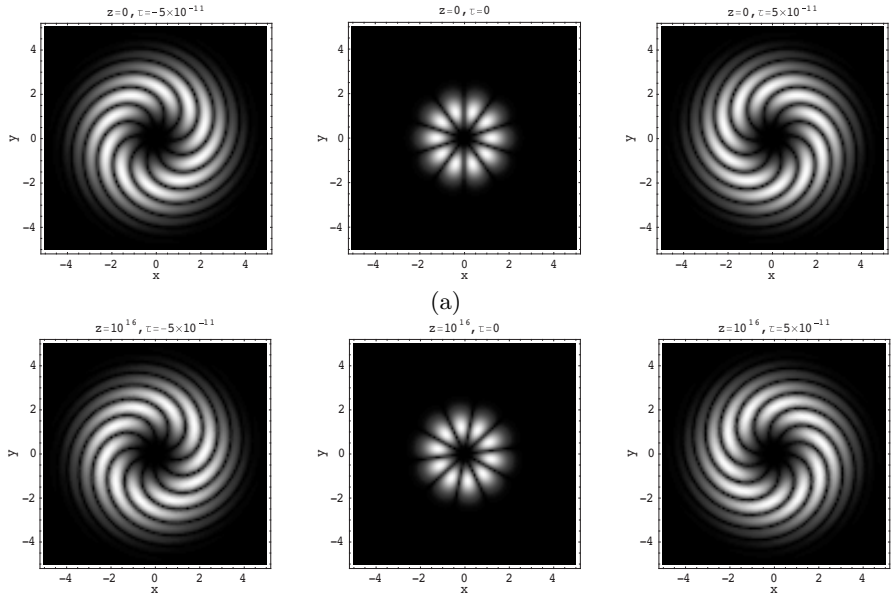

Figure 5. $|\vec{E}_x|$ vs. x, y for $\tau = -5 \times 10^{-11}, 0$ and 5×10^{-11} s at $z = 0$. (b) $|\vec{E}_x|$ vs. x, y for $\tau = -5 \times 10^{-11}, 0$ and 5×10^{-11} s at $z = 10^{16}$ m; Parameter values: $a_1 = 10^{-2}$ m, $a_2 = 1$, $a_3 = 1$ m, $b = 10^{14}$ m^{-1}, $p = 6 \times 10^{15}$, $q = 2$, and $m = 3$.

fields, the electromagnetic field energy density, shown in Fig. 7, is axisymmetric. The presence of an axial angular momentum is clearly seen in Fig. 8, which shows a plot of the electromagnetic momentum density $(1/c^2)\vec{E} \times \vec{H}$ vs. x, y for $\tau = -5 \times 10^{-11}, 0$ and 5×10^{-1} s on the aperture plane ($z = 0$).

4. CUNNINGHAM AND BATEMAN APPROACHES TO NULL ELECTROMAGNETIC PULSED BEAMS

4.1. Basic Riemann-Silberstein Electromagnetic Pulsed Beam Null Vector

4.1.1. The Cunningham Method

In the space-time frame $(\vec{R}_0, T_0)$, a specific solution to the nondimensionalized scalar wave equation (21) is chosen as follows:

$$\varphi(\vec{R}_0, T_0) = (Z_0 + T_0)^{-2}(X_0 + iY_0)/2. \tag{39}$$

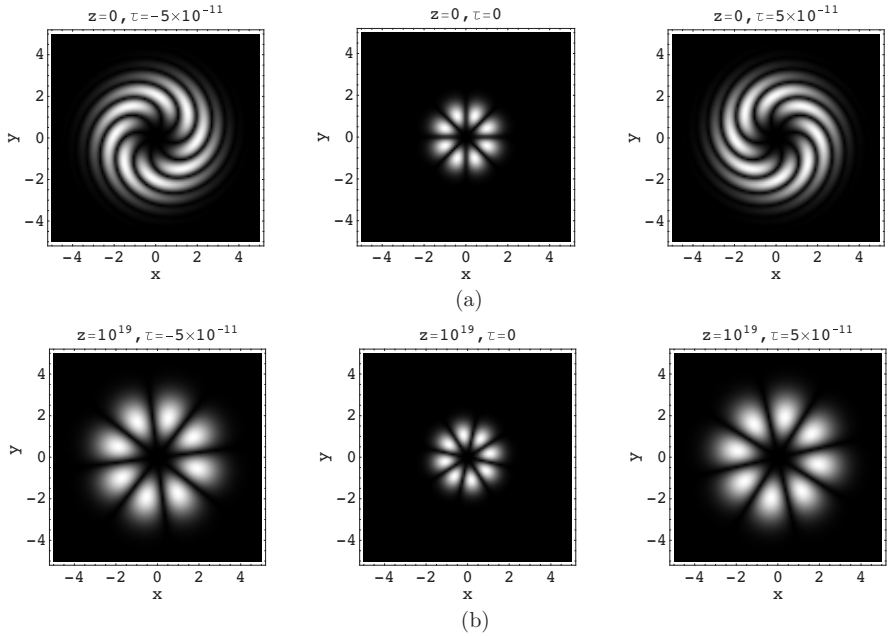

Figure 6. $|\vec{E}_z|$ vs. x, y for $\tau = -5 \times 10^{-11}, 0$ and 5×10^{-11} s at $z = 0$. (b) $|\vec{E}_z|$ vs. x, y for $\tau = -5 \times 10^{-11}, 0$ and 5×10^{-11} s at $z = 10^{19}$ m; Parameter values: $a_1 = 10^{-2}$ m, $a_2 = 1$, $a_3 = 1$ m, $b = 10^{14}\,\mathrm{m}^{-1}$, $p = 6 \times 10^{15}$, $q = 2$, and $m = 3$.

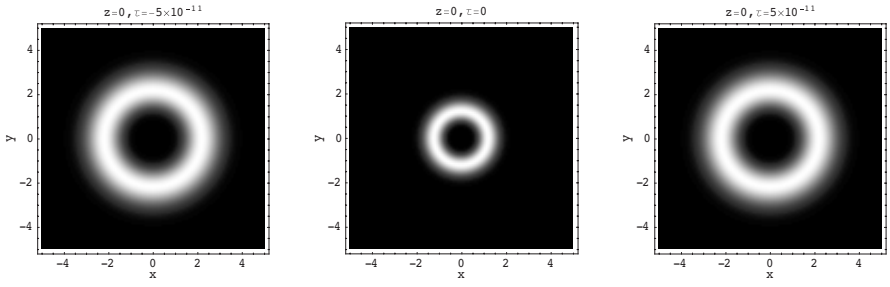

Figure 7. Electromagnetic field energy density w_{em} vs. x, y for $\tau = -5 \times 10^{-11}, 0$ and 5×10^{-11} s at $z = 0$; Parameter values: $a_1 = 10^{-2}$ m, $a_2 = 1$, $a_3 = 1$ m, $b = 10^{14}\,\mathrm{m}^{-1}$, $p = 6 \times 10^{15}$, $q = 2$, and $m = 3$.

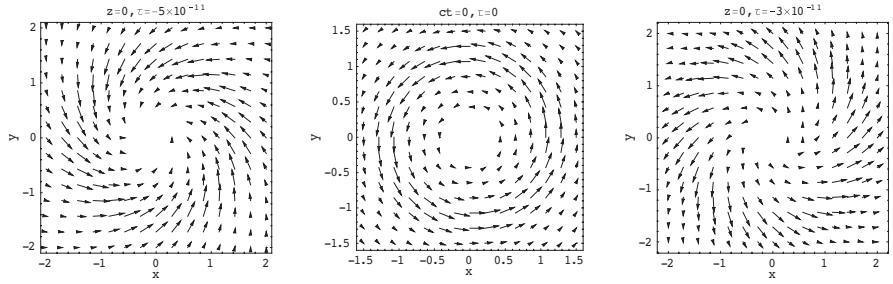

Figure 8. Parametric field plots of the x- and y-components of the electromagnetic momentum $(1/c^2)\vec{E}\times\vec{H}$ vs. x, y for $\tau = -3\times10^{-11}, 0$ and 3×10^{-11} s at $z = 0$; Parameter values: $a_1 = 10^{-2}$ m, $a_2 = 1$, $a_3 = 1$ m, $b = 10^{14}\,\mathrm{m}^{-1}$, $p = 6\times10^{15}$, $q = 2$, and $m = 3$.

Next, a vector-valued magnetic Hertz potential is defined as

$$\vec{\Pi}_m(\vec{R}_0, T_0) = \left\{0, 0, \varphi(\vec{R}_0, T_0)\right\}, \tag{40}$$

and the corresponding electromagnetic field intensities are computed:

$$\begin{aligned}
\vec{E}(\vec{R}_0, T_0) &= -\nabla_0\times\frac{\partial}{\partial T_0}\vec{\Pi}_m(\vec{R}_0, T_0) = \left\{\frac{i}{(Z_0+T_0)^3}, -\frac{1}{(Z_0+T_0)^3}, 0\right\},\\
\vec{H}(\vec{R}_0, T_0) &= \nabla_0\times\nabla_0\times\vec{\Pi}_m(\vec{R}_0, T_0) = \left\{-\frac{1}{(Z_0+T_0)^3}, -\frac{i}{(Z_0+T_0)^3}, 0\right\}.
\end{aligned} \tag{41}$$

According to the Cunningham formalism [cf. Eqs. (18) and (20)], the magnetic field intensity in the space-time frame $(\vec{r}_0, t_0)$ assumes the explicit form

$$\vec{h}(\vec{r}_0, t_0) = \left\{\begin{array}{l}
-\dfrac{(t_0 - x_0 + iy_0 + z_0)(t_0 + x_0 + iy_0 + z_0)}{(z_0+t_0)^3},\\
-i\dfrac{(t_0 + ix_0 - y_0 + z_0)(t_0 - ix_0 + y_0 + z_0)}{(z_0+t_0)^3},\\
2\dfrac{(x_0+iy_0)}{(z_0+t_0)^2}
\end{array}\right\}. \tag{42}$$

It should be noted that $\vec{h}\cdot\vec{h} = 0$. Furthermore, it turns out that $\vec{e} = i\vec{h}$. This means that $\vec{e}$ is also a null field. The space-time complexified [cf. Eq. (26)] version of the magnetic field given in Eq. (42) is the desired

basic Riemann-Silberstein electromagnetic pulsed beam null vector:

$$\vec{F}_{pb}(\vec{r},t) \equiv h(\vec{r},t) \left\{ \begin{array}{l} \dfrac{(x+iy)^2+(a_2-i(z+ct))^2}{(ia_2+z+ct)^3}, \\ -i\dfrac{(x+iy)^2-(a_2-i(z+ct))^2}{(ia_2+z+ct)^3}, \\ \dfrac{2(x+iy)}{(ia_2+z+ct)^2} \end{array} \right\} \tag{43}$$

4.1.2. The Bateman Method

In the space-time frame $(\vec{R}_0, T_0)$, a specific solution to the nondimensionalized scalar wave equation (21) is chosen as

$$\varphi(\vec{R}_0, T_0) = (Z_0 + T_0)(X_0 + iY_0), \tag{44}$$

and a vector-valued magnetic Hertz potential is defined as in Eq. (40). The subsequent procedure leading to the basic Riemann-Silberstein electromagnetic pulsed beam null vector is analogous to that followed in connection with the Cunningham approach, except that in the Bateman transformations given in Eq. (19), $z_0 - t_0$ must be replaced by $z_0 + t_0$.

4.2. Extended Null Luminal Localized Electromagnetic Pulsed Beams

Recall the definitions of the functions $\overline{\alpha}(\vec{r},t)$ and $\overline{\beta}(\vec{r},t)$ in Eq. (5), viz.,

$$\overline{\alpha}(\vec{r},t) \equiv a_1 + i(z-ct) + \frac{x^2+y^2}{a_2 - i(z+ct)},\ \overline{\beta}(\vec{r},t) \equiv \frac{x+iy}{a_2-i(z+ct)}. \tag{45}$$

Then, $\vec{G}(\vec{r},t) = \phi(\overline{\alpha},\overline{\beta})\vec{F}_{pb}(\vec{r},t)$ is a Riemann-Silberstein complex vector for any functional $\phi(\overline{\alpha},\overline{\beta})$ of $\overline{\alpha}(\vec{r},t)$ and $\overline{\beta}(\vec{r},t)$. Appropriate choices for $\phi(\overline{\alpha},\overline{\beta})$ give rise to finite-energy spatiotemporally localized electromagnetic pulsed beam real fields

$$\vec{E} = \sqrt{\frac{2}{\varepsilon_0}}\mathrm{Re}\left\{\vec{G}\right\}, \quad \vec{H} = \sqrt{\frac{2}{\mu_0}}\mathrm{Im}\left\{\vec{G}\right\}. \tag{46}$$

As a specific illustrative example, consider

$$\vec{G}(\vec{r},t) = \vec{F}_{pb}(\vec{r},t)\frac{1}{\overline{\alpha}^3}, \tag{47}$$

which is the pulsed beam analog of the Robinson-Troutman LW. The individual fields, the electromagnetic energy and momentum densities of these two localized structures differ significantly. It turns out, however, that the total energy and momentum of the real electromagnetic fields associated with the Riemann-Silberstein vector $G(\vec{r},t)$ in Eq. (47) are identical to those of the Robinson-Troutman electromagnetic null LW.

A number of graphical results are presented next in order to obtain a clearer view of some of the unique features of the null luminal electromagnetic pulsed beam incorporated into the Riemann-Silberstein vector $\vec{G}(\vec{r},t)$ in Eq. (47). The following notation is used: $\tau \equiv t - z/c$ is the local temporal coordinate around the pulse center; therefore, z is the distance from an "aperture" located at $z = 0$. The parameter values for all figures are $a_1 = 10^{-4}\,\mathrm{m}$ and $a_2 = 10^{4}\,\mathrm{m}$ Fig. 9(a) is a plot of $|E_x|$ vs. x, y for $\tau = -5 \times 10^{-11}, 0$ and $5 \times 10^{-11}\,\mathrm{s}$ on the aperture plane ($z = 0$). The "twisting" structure to the left and

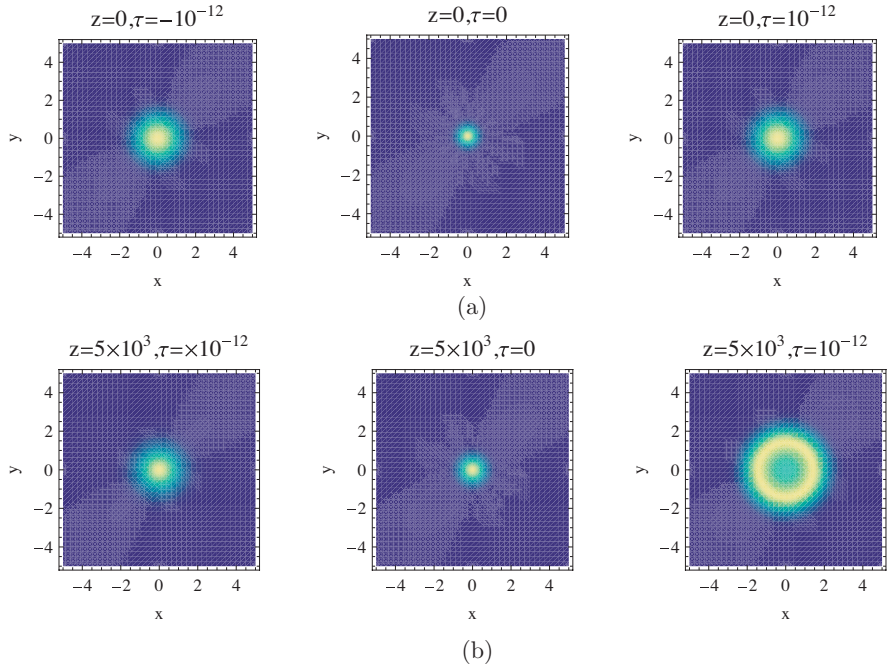

Figure 9. (a) $|\vec{E}_x|$ vs. x, y for $\tau = -8 \times 10^{-13}, 0$ and $8 \times 10^{-13}\,\mathrm{s}$ at $z = 0$. (b) $|\vec{E}_x|$ vs. x, y for $\tau = -8 \times 10^{-13}, 0$ and $8 \times 10^{-13}\,\mathrm{s}$ at $z = 5 \times 10^{3}\,\mathrm{m}$; Parameter values: $a_1 = 10^{-4}\,\mathrm{m}$, $a_2 = 10^{4}\,\mathrm{m}$.

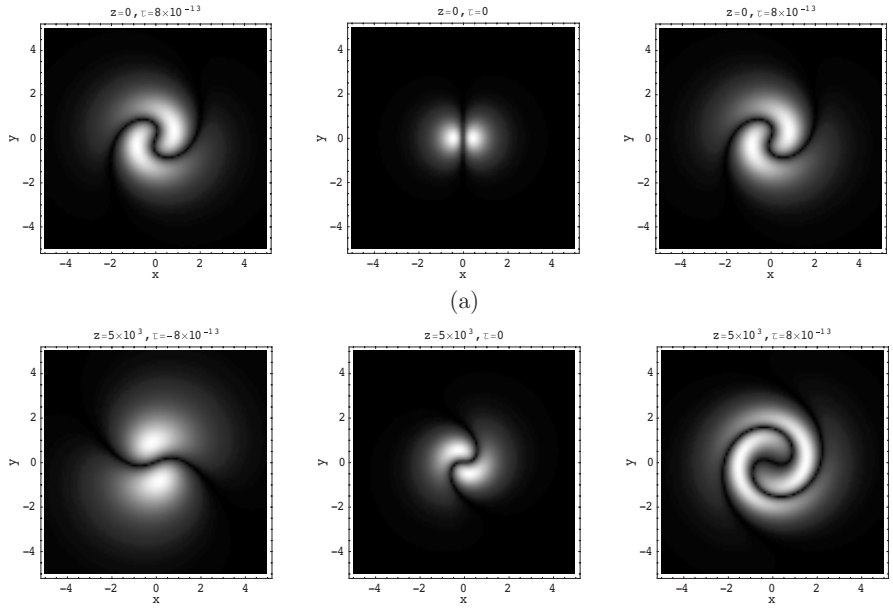

Figure 10. (a) $|\vec{E}_z|$ vs. x, y for $\tau = -8 \times 10^{-13}, 0$ and 8×10^{-13} s at $z = 0$. (b) $|\vec{E}_z|$ vs. x, y for $\tau = -8 \times 10^{-13}, 0$ and 8×10^{-13} s at $z = 5 \times 10^3$ m; Parameter values: $a_1 = 10^{-4}$ m, $a_2 = 10^4$ m.

the right of the pulse center present in the Robinson-Troutman LW is absent in this case. Fig. 9(b) is a plot of $|E_x|$ vs. x, y for $\tau = -10^{-11}, 0$ and 10^{-11} s at $z = 5 \times 10^3$ m. The different behavior at the pulse center and the loss of symmetry to the left and the right of the pulse center is due to the deformation of the wave packet as it propagates away from the aperture plane. The behavior of $|E_z|$ exhibited in Figs. 10(a) and 10(b) on the aperture plane and at $z = 5 \times 10^3$ m bears some similarity to that of the Robinson-Troutman LW. Despite the lack of azimuthal symmetry for the electromagnetic fields, the electromagnetic field energy density, shown in Fig. 11, is axisymmetric. The presence of an axial angular momentum is clearly seen in Fig. 12, which shows a plot of the electromagnetic momentum density $(1/c^2)\vec{E} \times \vec{H}$ vs. x, y for $\tau = -10^{-12}, 0$ and 10^{-12} s on the aperture plane ($z = 0$). The "twisting" of the momentum density field lines to the left and right of the pulse center present in the Robinson-Troutman LW is absent in the case of the pulsed beam.

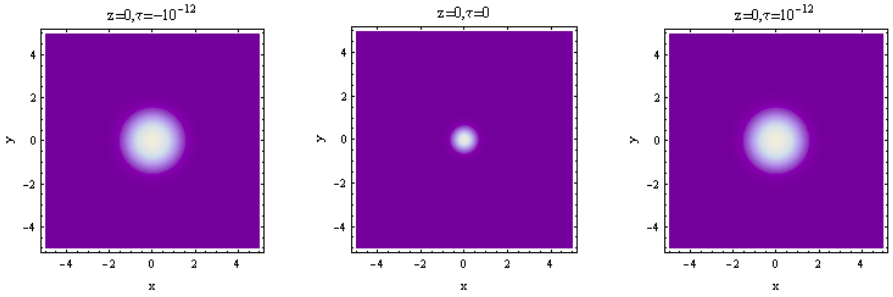

Figure 11. Electromagnetic field energy density w_{em} vs. x, y for $\tau = -10^{-12}, 0$ and 10^{-12} s at $z = 0$. Parameter values: $a_1 = 10^{-4}$ m, $a_2 = 10^4$ m.

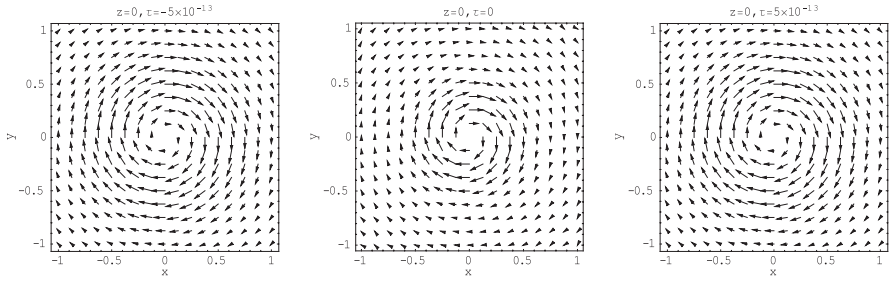

Figure 12. Parametric field plots of the x- and y-components of the electromagnetic momentum $(1/c^2)\vec{E} \times \vec{H}$ vs. x, y for $\tau = -5 \times 10^{-13}, 0$ and 5×10^{-13} s at $z = 0$. Parameter values: $a_1 = 10^{-4}$ m, $a_2 = 10^4$ m.

5. CONCLUDING REMARKS

Ordinarily, one derives a luminal electromagnetic LW using the Hertz vector potential method. Specifically, an arbitrary scalar-valued luminal LW $\psi(\vec{r}, t)$ of the general form given in Eq. (2) is used to form magnetic and electric vector Hertz potentials

$$\vec{\Pi}_{m,e}(\vec{r}, t) = \{0, 0, \psi(\vec{r}, t)\}. \tag{48}$$

Then, transverse electric (TE) and transverse magnetic (TM) luminal electromagnetic LWs are obtained as follows:

$$\begin{aligned} \vec{e}_m(\vec{r}, t) &= -\mu_0 \nabla \times \frac{\partial}{\partial t} \vec{\Pi}_m(\vec{r}, t), \ \vec{h}_m(\vec{r}, t) = \nabla \times \nabla \times \vec{\Pi}_m(\vec{r}, t); \\ \vec{e}_e(\vec{r}, t) &= \nabla \times \nabla \times \vec{\Pi}_e(\vec{r}, t), \ \vec{h}_e(\vec{r}, t) = \varepsilon_0 \nabla \times \frac{\partial}{\partial t} \vec{\Pi}_e(\vec{r}, t). \end{aligned} \tag{49}$$

Of course, superpositions of these fields, e.g.,

$$\vec{e}(\vec{r},t) = \vec{e}_e(\vec{r},t) + \vec{e}_m(\vec{r},t),\ \vec{h}(\vec{r},t) = \vec{h}_e(\vec{r},t) + \vec{h}_m(\vec{r},t), \tag{50}$$

are also complex-valued luminal localized solutions to Maxwell's equations. Due to the complexity of the scalar-valued LW $\psi(\vec{r},t)$ entering into the vector Hertz potentials, and the ensuing spatio-temporal differentiations in Eq. (49), the resulting electromagnetic fields are, in general, quite complicated and questions regarding total energy, momentum, and angular momentum content become nontrivial.

Some of the aforementioned complexity is alleviated in the case of null luminal electromagnetic LWs because a Riemann-Silberstein complex vector associated with such structures is given by $\vec{F}(\vec{r},t) = \vec{f}_b(\vec{r},t)\psi(\vec{r},t)$; in other words, it is defined as the product of the basic complex-valued vector defined in Eq. (14) and an arbitrary scalar LW of the general form given in Eq. (2). Since no differentiation is involved, the structures of $\vec{F}(\vec{r},t)$ and the corresponding real electric and magnetic fields $\vec{E}(\vec{r},t)$ and $\vec{H}(\vec{r},t)$ are relatively simple, thus facilitating the explicit computations of the total energy and angular momentum they carry.

Suppose a scalar luminal LW $\psi(\vec{r},t)$ contains finite energy within the framework of a scalar wave theory. This does not necessarily mean that the real electromagnetic fields associated with the Riemann-Silberstein complex vector $\vec{F}(\vec{r},t) = \vec{f}_b(\vec{r},t)\psi(\vec{r},t)$ also contain finite energy. Consider, for example, the first-order splash mode

$$\psi^{(1)}_{sm}(\vec{r},t) = \frac{1}{a_1 + i(z-ct)}\frac{1}{\alpha(\vec{r},t)}. \tag{51}$$

It contains finite energy within the framework of a scalar wave theory. Furthermore, it has been shown by Feng et al. [34] and more recently by Lekner [35] that either the TE or TM electromagnetic fields obtained from the aforementioned vector Hertz potential theory contain finite energy. In contradistinction, the real electromagnetic fields associated with the null Riemann-Silberstein complex vector $\vec{F}(\vec{r},t) = \vec{f}_b(\vec{r},t)\psi^{(1)}_{sm}(\vec{r},t)$ contain infinite energy. However, the Robinson-Troutman null Riemann-Silberstein complex vector $\vec{F}_{RT}(\vec{r},t) = \vec{f}_b(\vec{r},t)\psi^{(3)}_{sm}(\vec{r},t)$, where

$$\psi^{(3)}_{sm}(\vec{r},t) = \frac{1}{a_1 + i(z-ct)}\frac{1}{\alpha^3(\vec{r},t)} \tag{52}$$

is the third-order scalar splash mode, leads to real electromagnetic fields containing finite energy.

There exist classes of luminal scalar LWs which do not conform to the template given in Eq. (2). A particular example is the Bessel-Gauss FWM

$$\psi_{BG}(\vec{r},t) = \frac{1}{a_1 + i(z-ct)} \exp[-ik\alpha(\vec{r},t)] \times \exp\left[-\frac{p^2}{k}\frac{1}{a_1+i(z-ct)}\right] I_0\left[p\frac{\sqrt{x^2+y^2}}{a_1+i(z-ct)}\right], \quad (53)$$

which was introduced by Shaarawi [36] and subsequently studied by Overfelt [37]. In this expression, k and p are free parameters, with units m^{-1}, and $I_0(\cdot)$ is the zero-order modified Bessel function. For $p = 0$, $\psi_{BG}(\vec{r},t)$ reduces to the FWM [1, 2, 4], which, in addition to the splash modes, is one of the simplest solutions conforming to the template given in Eq. (2). The general theory of null luminal localized electromagnetic waves developed in this article does not apply to the Bessel-Gauss FWM. In other words, $\vec{F}(\vec{r},t) = \vec{f}_b(\vec{r},t)\psi_{BG}(\vec{r},t)$ is not a null Riemann-Silberstein complex vector. Basically, this is due to the fact that, in general, a superposition of null vectors is not a null vector.

Wave packets carrying angular momentum and characterized by vortex structures are of physical importance and are being intensely studied in several areas, e.g., optical vortices [38–42], photon entanglement [43], etc. The systematic exposition of exact spatiotemporally localized luminal null electromagnetic waves introduced in this article is relevant and should prove useful in this direction.

The discussion is this article has been confined to spatiotemporally localized luminal null electromagnetic waves. In a sequel to this article, appropriate choices of functions $\alpha(\vec{r})$ and $\beta(\vec{r})$, analogous to but distinct from those defined in Eq. (2), together with the Whittaker-Bateman potential theory and the Lorentz transformations of Maxwell's equations, will allow us to report on a novel wide class of spatiotemporally localized superluminal null electromagnetic waves.

REFERENCES

1. Brittingham, J. N., "Focus wave modes in homogeneous Maxwell equations: Transverse electric mode," *J. Appl. Phys.*, Vol. 54, 1179–1189, 1983.
2. Kiselev, A. P., "Modulated Gaussian beams," *Radio Phys. Quant. Electron.*, Vol. 26, 1014, 1983.

3. Belanger, P. A., "Packetlike solutions of the homogeneous wave equation," *J. Opt. Soc. A*, Vol. 1, 723, 1984.
4. Ziolkowski, R. W., "Exact solutions of the wave equation with complex source locations," *J. Math. Phys.*, Vol. 26, 861–863, 1984.
5. Ziolkowski, R. W., "Localized transmission of electromagnetic energy," *Phys. Rev. A*, Vol. 39, 2005–2033, 1989.
6. Besieris, I. M., A. M. Shaarawi, and R. W. Ziolkowski, "A bidirectional traveling plane wave representation of exact solutions of the scalar wave equation," *J. Math. Phys.*, Vol. 30, 1254–1269, 1989.
7. Ziolkowski, R. W., I. M. Besieris, and A. M. Shaarawi, "Localized wave representations of acoustic and electromagnetic radiation," *Proc. IEEE*, Vol. 79, 1371–1378, 1991.
8. Grunwald, R., V. Kebbel, U. Griebner, U. Neumann, A. Kummrow, M. Rini, E. T. Nibbering, M. Piche, G. Rousseau, and M. Fortin, "Generation and characterization of spatially and temporally localized few-cycle optical wave packets," *Phys. Rev. A*, Vol. 67, 063820, 1–5, 2003.
9. Ziolkowski, R. W., D. K. Lewis, and B. D. Cook, "Experimental verification of the localized wave transmission effect," *Phys. Rev. Lett.*, Vol. 62, 147–150, 1989.
10. Ziolkowski, R. W. and D. K. Lewis, "Verification of the localized wave transmission effect," *J. Appl. Phys.*, Vol. 68, 6083–6086, 1990.
11. Reivelt, K. and P. Saari, "Experimental demonstration of realizability of optical focus wave modes," *Phys. Rev. E*, Vol. 66, 056611-1-9, 2002.
12. Courant, R. and D. Hilbert, *Methods of Mathematical Physics*, Vol. II, Interscience, New York, 1962.
13. Hillion, P., "Courant-Hilbert solutions of the wave equation," *J. Math Phys.*, Vol. 33, 34–45, 1992.
14. Bateman, H., "The conformal transformations of four dimensions and their applications to geometrical optics," *Proc. London Math. Soc.*, Vol. 7, 70–89, 1909.
15. Bateman, H., *The Mathematical Analysis of Electrical and Optical Wave-Motion on the Basis of Maxwell's Equations*, Dover, New York, 1955.
16. Borisov, V. V. and A. B. Utkin, "Generalization of Brittingham's localized solutions to the wave equation," *Euro. Phys. J. B*, Vol. 21, 477–480, 2001.
17. Kiselev, A. P., "Generalization of Bateman-Hillion progressive

wave and Bessel-Gauss pulse solutions to the wave equation," *J. Phys. A: Math. Gen.*, Vol. 36, L345–L349, 2003.

18. Besieris, I. M. and A. M. Shaarawi, "Bateman conformal transformations within the framework of the bidirectional spectral representation," *Progress In Electromagnetics Research*, PIER 48, 201–231, 2004.
19. Ziolkowski, R. W., I. M. Besieris, and A. M. Shaarawi, "Aperture realizations of the exact solutions to homogeneous-wave equations," *J. Opt. Soc. Am. A*, Vol. 10, 75–87, 1993.
20. Shaarawi, A. M., I. M. Besieris, R. W. Ziolkowski, and S. M. Sedky, "Generation of approximate focus wave mode pulses from wide-band dynamic Gaussian aperture," *J. Opt. Soc. Am. A*, Vol. 12, 1954–1964, 1995.
21. Kiselev, A. P. and M. V. Perel, "Highly localized solutions of the wave equation," *J. Math. Phys.*, Vol. 41, 1934–1955, 2000.
22. Heyman, E., "Pulsed beam propagation in an inhomogeneous medium," *IEEE Trans. Antennas Propag.*, Vol. 42, 311–319, 1994.
23. Cunningham, E., "The principle of relativity in electrodynamics and an extension thereof," *Proc. London Math. Soc.*, Vol. 8, 77–98, 1909.
24. Bateman, H., "The transformation of the electrodynamical equations," *Proc. London Math. Soc.*, Vol. 8, 223–264, 1910.
25. Bateman, H., "The transformations of coordinates which can be used to transform one physical problem into another," *Proc. London Math. Soc.*, Vol. 8, 469–488, 1910.
26. Robinson, I., "Null electromagnetic fields," *J. Math. Phys.*, Vol. 2, 290–291, 1961.
27. Robinson, I. and A. Troutman, "Some spherical gravitational waves in general relativity," *Proc. R. Soc. London*, Series A, 265, 463, 1962.
28. Robinson, I. and A. Troutman, *New Theories in Physics: Roc. Warsaw Symp. On Elementary Particle Physics*, Z. Ajduk et al. (eds.), 454–497, Singapore World Scientific, 1989.
29. Troutman, A., "Robinson manifolds and Cauchy-Riemann spaces," *Class. Quantum Grav.*, Vol. 19, R1–R10, 2002.
30. Penrose, R. and W. Rindler, *Spinors and Space-Time*, Vol. 2, Cambridge University Press, 1986.
31. Bialynicki-Birula, I., "Electromagnetic vortex lines riding atop null solutions of the Maxwell equations," *J. Opt. A: Pure Appl. Opt.*, Vol. 6, S181–S183, 2004.
32. Weber, H., *Die Partiellen Differential-Gleichungen der Mathema-*

tischen Physik nach Riemann's Vorlesungen, Friedrich Vieweg und Sohn, Brunschweig, 1901.

33. Silberstein, L., "Electromagnetische grundgleichungen in bivectorieller behandlung," *Ann. d. Phys.*, Vol. 22, 579–586, 1907.
34. Feng, S., H. G. Winful, and R. W. Hellwarth, "Spatio-temporal evolution of single-cycle electromagnetic pulses," *Phys. Rev. E*, Vol. 59, 4630–4649, 1999.
35. Lekner, J., "Energy and momentum of electromagnetic pulses," *J. Opt. A: Pure Appl. Opt.*, Vol. 6, 146–147, 2004.
36. Shaarawi, A. M., "Nondispersive wavepackets," Ph.D. Thesis, Virginia Polytechnic Inst. and State Univ., 1989.
37. Overfelt, P., "Bessel-Gauss pulses," *Phys. Rev. A*, Vol. 44, 3941–3947, 1991.
38. Bialynicki-Birula, I. and Z. Bialynicki-Birula, "Vortex lines of the electromagnetic field," *Phys. Rev. A*, Vol. 67, 062114-1, 2003.
39. Berry, M., "Riemann-Silberstein vortices for paraxial waves," *J. Opt. A: Pure Appl. Opt.*, Vol. 6, S175-7, 2003.
40. Kaiser, G., "Helicity, polarization and Riemann-Silberstein vortices," *J. Opt. A: Pure Appl. Opt.*, Vol. 6, S243-5, 2003.
41. Lekner, J., "Helical light pulses," *J. Opt. A: Pure Appl. Opt.*, Vol. 6, L29–L32, 2004.
42. Desyatnikov, A. S., Y. S. Kivshar, and L. Torner, "Optical vortices and vortex solitons," *Progress in Optics*, E. Wolf (ed.), Vol. 47, 291–391, North-Holland, 2005.
43. Molina-Terriza, G., J. P. Torres, and L. Torner, "Management of the angular momentum of light; preparation of photons in multidimensional vector states of angular momentum," *Phys. Rev. Lett.*, Vol. 88, 0136011-4, 2002.